J Porous Mater (2017) 24:881–886
DOI 10.1007/s10934-016-0327-4

Synthesis of silicate-1 monolith and its catalytic application

Xiaobing Yang[1] · Liuqing Huang[1] · Guiqing Du[1] · Xuetao Lu[1]

Published online: 21 November 2016

Abstract Silicate-1 monolith was facilely synthesized in the precursor solution by combining sol–gel method and hydrothermal method. Characterization by X-ray diffraction, Fourier transform infrared spectroscopy, scanning electron microscopy and transmission electron microscope revealed that silicate-1 particles were formed by transforming amorphous SiO_2 into MFI-type structure and inlayed into the three-dimensional network of silica to form the monolith. Then, silicate-1 monolith was used as support to load TiO_2 by dip-coating method. TiO_2 nanoparticles were well dispersed in silicate-1 monolith. The photocatalytic properties of all samples were evaluated based on the degradation efficiency of Rhodamine B. And a scheme regarding photodegradation enhancement induced by dye enrichments has been proposed to illustrate the adsorption-photodegradation process.

Keywords Silicate-1 monolith · TiO_2-loaded silicate-1 monolith · Catalytic activity

1 Introduction

Zeolites, as one of a porous material, have high surface areas, excellent hydrothermal stability, controllable porosity and acid/basic/redox properties. It is composed of SiO_4 and AlO_4 tetrahedral structure and has been widely used as adsorbents [1], ion exchangers and catalysts in chemical industry [2, 3]. Until now, many zeolites have been discovered, such as MCM-41 [4], 5A [5], zeolite Y [6], and ZSM-5 [7].

In the traditional research, zeolites are generally synthesized as powders. In order to be more convenience for catalytic and adsorbent applications, zeolite powders are always shaped into monolith. The traditional technology for producing zeolite monolith involves introducing additives to allow the compression of powders, such as clays (bentonite [8], attapulgite [9]), silica based compounds (tetraethylorthosilicate [10], colloidal silica [11]) or aluminum base compounds (alumina [12]). Zeolite powders are dispersed homogeneously with binder, and then treated by a drying and heating step. Zeolite powders are bonded together by binder, but the existence of additive reduces their surface area. Moreover, binders can be responsible for negative effects like the blocking of micropores and active sites or the incorporation of other atoms in the zeolitic framework [8, 12]. Hence, it is necessary to prepare the zeolite monoliths with less of binder and a high mechanical resistance.

Recently, there are appearing several new methods to prepare zeolite monoliths, such as spark plasma sintering [13–15], slip casting [16], and hydrothermal hot pressing method [17]. Some of the used methods in the conception of bodies are handled by the extrusion process, which leads to the formation of monoliths amongst others. The others are processed in cylinder by a rapid powder processing method [18]. However, the amount of binder the mechanical resistance is either high or the mechanical resistance is still low for each of these methods. And all of these processes need to synthesize zeolite firstly, and then convert zeolite powders into zeolite monolith. The processes are complicated and energy-consuming.

Silicate-1, as one of zeolite, is widely used in many fields, such as styrene epoxidation [19], esterification

✉ Xuetao Lu
xuetao@xmu.edu.cn

[1] Fujian Key Laboratory of Advanced Materials, College of Materials, Xiamen University, Xiamen 361005, China

reaction [20], and hydrocracking of residual oil [21]. In this work, we demonstrate sol–gel method for one-step synthesis of silicate-1 monolith from the precursor solution without the use of any secondary binders. It is easy to be used and takes less time than the previous methods. In this investigation, the precursor solution gelled quickly after it was removed into Teflon-lined autoclave for hydrothermal reaction, in which the water molecule and silica particles were immobilized in the three-dimensional net structure and loses its mobility [22]. And silicate-1 grains formed in the gelatin and grew up by transferring the silica gelatin into silicate-1 structure. The redundant silica could bond silicate-1 particles together in its three-dimensional (3D) network. After that, the monolith was dried and calcined in the air to remove the water and TPABr. Finally, silicate-1 monolith was used as supporter to synthesize the TiO_2-loaded silicate-1 monolith by dip-coating method [23]. And its photocatalytic activity was investigated by the photocatalytic degradation of RhB.

2 Experimental

2.1 Chemicals

Silica sol (30 wt%, pH = 9.46) was obtained from Jiyida silica reagent factory. Sodium hydroxide, tetrabutyl titanate, absolute ethanol, acetic acid, nitric acid and tetrapropyl ammonium bromide (TPABr) were purchased from Sinopharm Chemical Reagent Co. Ltd. All chemicals were used without any further purification.

2.2 Synthesis of silicate-1 monolith

Silicate-1 monolith was directly synthesized in a eutectic mixture. Silica sol (30 wt%, pH = 9.46) was used as silicon source. The precursor solution of silicate-1 monolith was composed of tetrapropyl ammonium bromide, sodium hydroxide and silica sol with the ratio of 1.5 g: 0.2 g: 30 ml. It was vigorously stirred for 2 h at room temperature. After that, the solution was transferred into the Teflon-lined stainless-steel autoclave and crystallized at 180 °C for 24 h to form the silicate-1 monolith. The schematic diagram of the synthestic procedure of silicate-1 monolith and the synthesized monolith are shown in Fig. 1. The obtained gelatinous monolith was dried at 60 °C for 24 h. Then, the monolith was calcined at 550 °C for 6 h to remove the templates.

2.3 Preparation of TiO_2-coated silicate-1 monolith

Silicate-1 monolith was used as substrates to support nanocrystalline TiO_2 by the sol–gel method. Precursor solution for the TiO_2 sol was prepared as follows: tetrabutyl titanate (11.2 mL) and diethanolamine (3.8 mL) were dissolved in 30 mL of ethanol. The solution was stirred vigorously at room temperature, followed by the addition of a mixture of distilled water (4.5 mL), ethanol (10 mL) and hydrochloric acid (30 wt%, 0.5 mL). The resulting alkoxide solution was left at room temperature to hydrolyze for a period of time to obtain a TiO_2 sol. Silicate-1 monolith was immersed into the TiO_2 sol. When the monolith was saturated with TiO_2 sol, the TiO_2 sol-coated monolith was dried at drying oven and, subsequently, the process was repeated from immersion to drying for five times. Finally, the dried TiO_2-sol coated monolith was calcined at 500 °C in air for 2 h.

2.4 Characterization and test

The morphology of samples was observed using scanning electron microscopy (SEM) on Hitachi TM3000 microscope. The X-ray powder diffraction patterns of the ground monoliths were recorded on a Bruker-AxsD8 diffractometer. Fourier transform infrared spectroscopy (FT-IR) was characterized from 400 to 4000 cm-1 resolution on a Thermo Scientific N[1]icolet iS10. The nitrogen adsorption–desorption isotherm were recorded using TriStar 3020 (Micromeritics, USA) analyzer. The monoliths were grounded into powders and degassed at under vacuum at 250 °C for 2 h and adsorption and desorption data were collected at −196 °C. The specific surface areas were calculated using the multiple-point Brunauer–Emmetl–Teller (BET) method by the Barrett–Joyner–Halenda (BJH) model. The micropore size distribution was measured using the Horvath–Kawazoe (HK) analysis method.

2.5 Catalytic evaluation

The catalytic performance of TiO_2-coated silicate-1 monolith was evaluated by degradation of Rhodamine B (RhB) solution in an inclosed box with side the volume of $28 \times 28 \times 28$ cm^3. A Philips lamp irradiating UV light with the power of 40 W was fixed on the top of the box. And a magnetic stirrer was located at the bottom of the box. When the catalyst was used in the degradation measurement, it was ground into powders and mixed in the aqueous solution containing RhB. In each experiment, 100 ml rhodamine B aqueous solution (5 mg/L) containing 0.1 g catalyst was put into the reactor. In prior of UV light irradiation, the solution was stirred continuously in the dark for 30 min to ensure the adsorption–desorption equilibrium between RhB and the catalyst. Afterwards, the UV light was turned on and the solution was irradiated for 90 min. In order to determine the residual dye concentration in solution during this time, a few milliliters of the solution

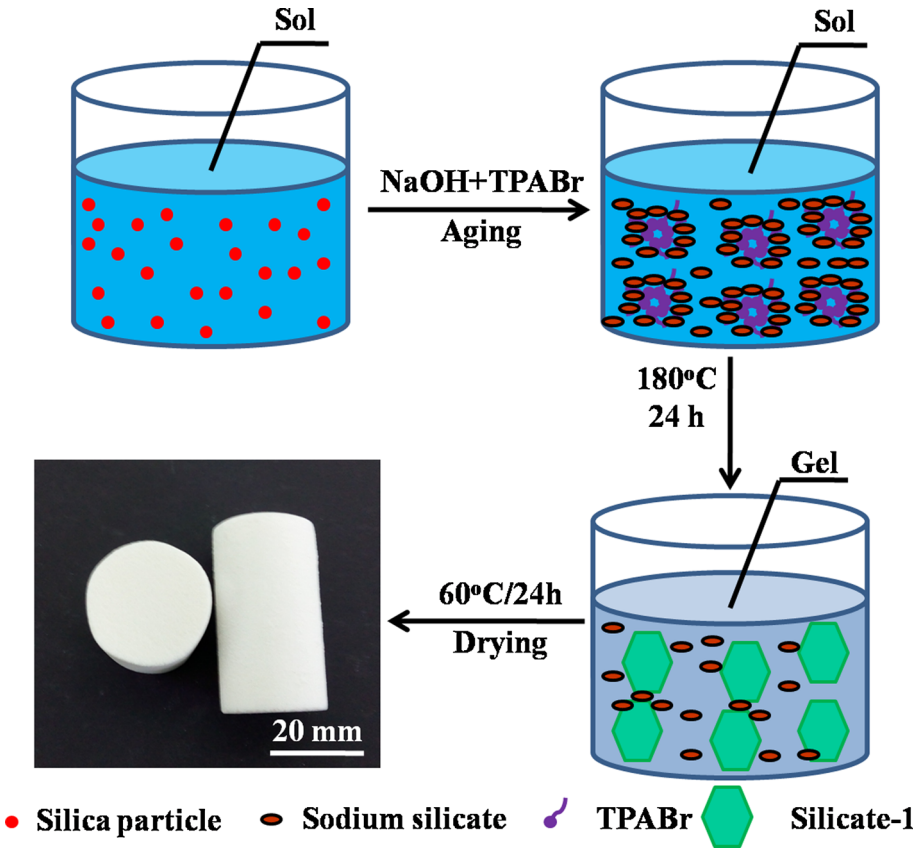

Fig. 1 Schematic diagram of the synthetic procedure and the synthesized silicate-1 monolith

was withdrawn from the reactor and centrifuged to remove the photocatalyst before measuring. The fractional degradation efficiency (D_R) of RhB was calculated by the following equation:

$$D_R(\%) = \frac{(C_0 - C_t)}{C_0} * 100$$

where C_o is the initial concentration of RhB and C_t is the concentration at definite interval of time, respectively.

3 Results and discussion

Silicate-1 monolith was synthesized by sol–gel method. We used silica sol (30 wt%, pH = 9.54) as silicon source to synthesize silicate-1 monolith. The precursor solution was composed with 30 ml silica sol, 0.2 g NaOH, and 1.5 g TPABr. It was aged for 2 h at room temperature and crystallized at 180 °C for 24 h. Figure 2 shows the SEM images of silicate-1 monolith and TiO_2-loaded silicate-1 monolith. It can be seen that silicate-1 grains are formed with the uniform particle sizes about 25 μm. Silicate-1 grains are bonded together by amorphous SiO_2 (Fig. 2a). Figure 2b is the SEM image of TiO_2-loaded silicate-1 monolith. It is almost the same with silicate-1 monolith.

The XRD patterns of silicate-1 monolith and TiO_2-loaded silicate-1 monolith are shown in Fig. 3. It can be seen that both of two samples show five distinct peaks at 7.98°, 8.82°, 23.18, 24.02°, and 24.46°, which is corresponding to (101), (020), (503), (151), and (303) reflections of MFI-type structure, respectively [24, 25]. When silicate-1 monolith is loads with TiO_2, it shows five new peaks at 25.23°, 37.82°, 48.05° and 53.91°, which is ascribable to (101), (112), (200) and (105) reflections of anatase [26–28]. It indicates that TiO_2 is well loaded on silicate-1 monolith.

Figure 4 is the FT-IR spectra of silicate-1 monolith and TiO_2-loaded silicate-1 monolith. From Fig. 4, it can be seen that both of samples show five absorption peaks at 475, 546, 795, 950, and 1119 cm^{-1}. The bands at 1119 and 795 cm^{-1} are ascribable to the internal asymmetric stretching vibration and external symmetric stretching of Si–O–Si bonds, respectively [24]. The stretching vibration of the Si–OH group is shown at 950 cm^{-1}. The band at around 546 cm^{-1} is attributed to the five membered ring of pentasil zeolite structure [29]. The band at 475 cm^{-1} is due to the bending vibration of SiO_4. When silicate-1 monolith is loaded with TiO_2, it shows a wide band from 504 to 657 cm^{-1}, which is corresponding to the absorption bond of Ti–O–Ti [29].

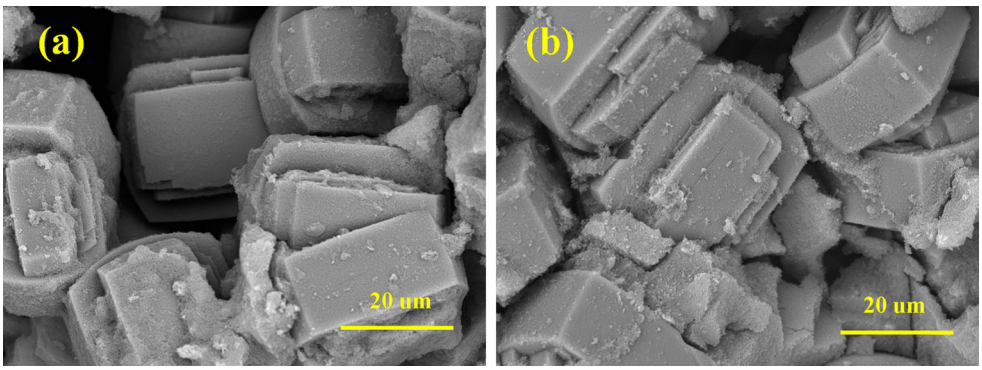

Fig. 2 SEM images of **a** silicate-1 monolith and **b** TiO_2-loaded silicate-1 monolith

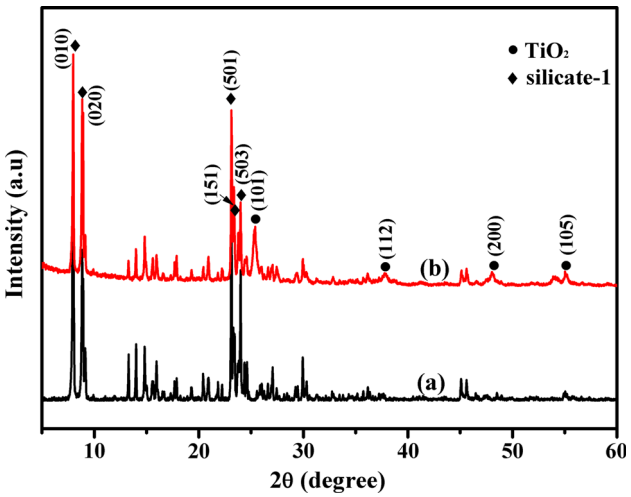

Fig. 3 XRD patterns of **a** silicate-1 monolith and **b** TiO_2-loaded silicate-1 monolith

In the preparation of TiO_2-loaded silicate-1 monolith, we used the silicate-1 monolith as support. The synthetic procedure is given as above. Figure 5 shows that diffuse reflectance UV–Vis spectra of silicate-1 monolith and TiO_2-loaded silicate-1 monolith. It can be seen that the TiO_2-loaded silicate-1 monolith catalyst exhibits a highly intense band at about 388 nm. According to the Kubelka–Munk radiative transfer model, the band gap (E_g) of TiO_2-loaded silicate-1 is about 3.2 eV. It indicates that TiO_2 is successfully loaded in silicate-1 monolith.

The TEM images of silicate-1 monolith and TiO_2-loaded silicate-1 monolith are shown in Fig. 6. Figure 6a is the TEM image of silicate-1 monolith. It can be seen that the surface of silicate-1 monolith is composed of amorphous SiO_2. After silicate-1 monolith is dip-coating with TiO_2, it shows the lattice fringes of anatase. It indicates that TiO_2 nanoparticles are well loaded in silicate-1 monolith.

The catalytic performance of the prepared TiO_2-loaded silicate-1 monolith was examined by degradation of RhB.

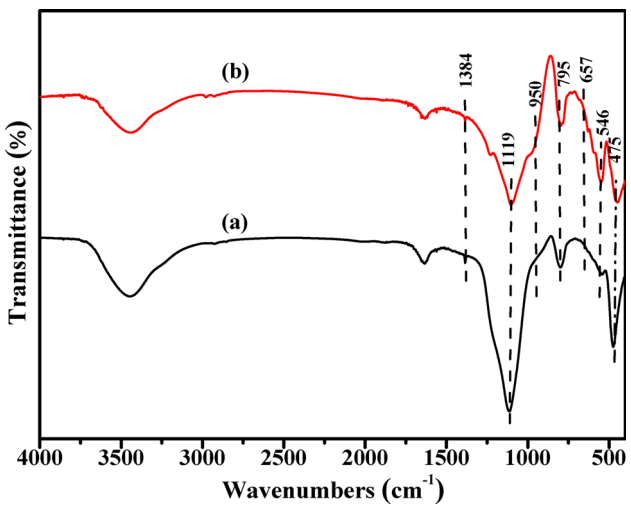

Fig. 4 FT-IR spectra of **a** silicate-1 monolith and **b** TiO_2-loaded silicate-1 monolith

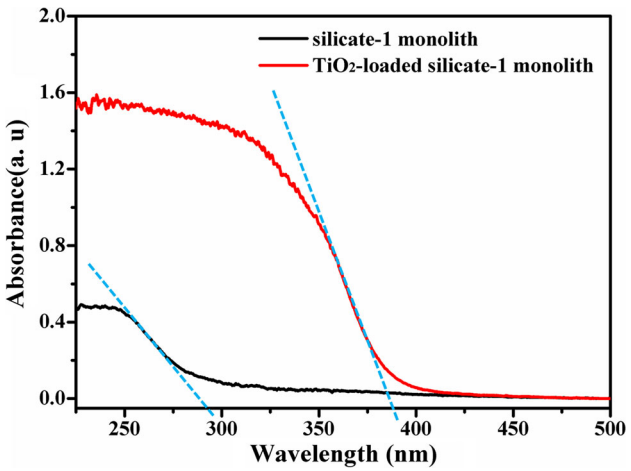

Fig. 5 UV–Vis spectra of silicate-1monolith and TiO_2-loaded silicate-1 monolith

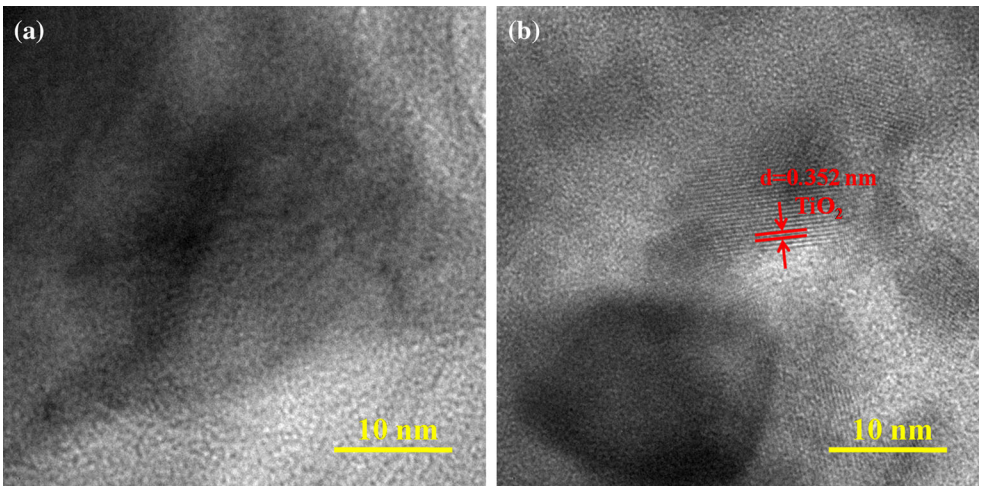

Fig. 6 TEM images of **a** silicate-1 monolith and **b** TiO_2-loaded silicate-1 monolith

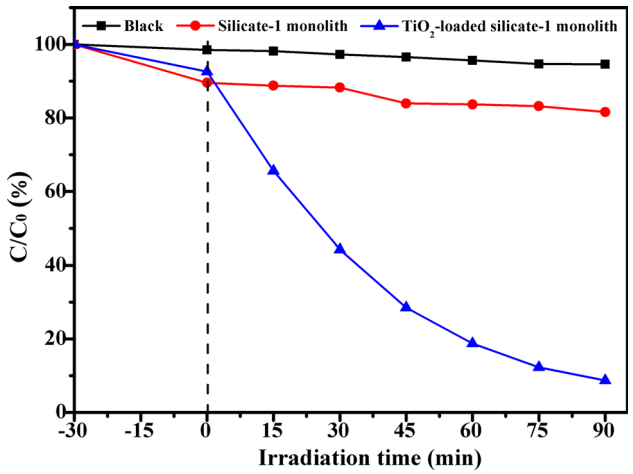

Fig. 7 Photocatalytic degradation of RhB solution in the dark and under UV light irradiation with a catalyst content of 1 g L^{-1}, $C_0 = 5$ mg L^{-1}

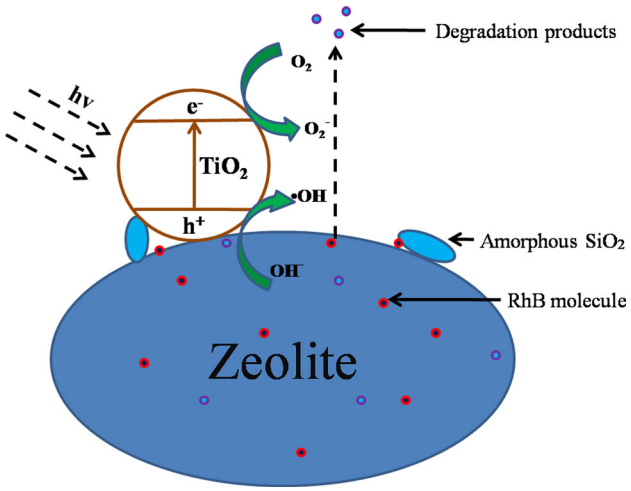

Fig. 8 The schematic diagram for the adsorption and photocatalytic degradation of RhB molecules on catalyst

Figure 7 shows the results of RhB removal by the catalysts. After 30 min of continuously stirring in the dark, 10.4% of RhB is absorbed by silicate-1 monolith. And TiO_2-loaded silicate-1 monolith shows 7.4% absorption. The adsorptive property of the catalyst is reduced, which is contributed to the loading of TiO_2 in the pores of silicate-1 monolith. Then, all experiments are exposed under the UV light for 90 min. From Fig. 7, we can see that 3.9% of RhB is degraded by itself under the UV light. The existing of silicate-1 monolith powders cannot accelerate the degradation of RhB. After silicate-1 monolith is loaded with TiO_2 particles, its photocatalytic efficiency is about 91.4%. The catalyst shows high photocatalytic activity after silicate-1 monolith is loaded with TiO_2.

Figure 8 shows the schematic diagram for the adsorption and photocatalytic degradation of RhB molecules on catalyst. Silicate-1 zeolite has high adsorptive property. It can keep a high RhB concentration on its surface for its adsorption. There is an adsorption–desorption equilibrium between the catalyst and the solution. When TiO_2 particles are immobilized on silicate-1 and irradiated by UV light, it can generate the hydroxyl radicals and valence band holes to oxidize RhB molecules into inorganic compounds. The adsorption of the zeolites and photocatalysis of the deposited TiO_2 have been combined, resulting in synergistic effects in improving the photocatalytic efficiency of TiO_2.

4 Conclusions

We demonstrated a facile and practical method to fabricate silicate-1 monolith. Silicate-1 grains are formed by transforming amorphous SiO_2 into MFI type structure and

bonded together by excess amorphous SiO_2. And TiO_2-loaded silicate-1 monolith, using silicate-1 monolith as support, was also successfully prepared by dip-coating method. TiO_2 nanoparticles were well loaded in silicate-1 monolith. It exhibited high catalytic performance for degradation of RhB. This study opens a new possibility in the investigation of TiO_2-silicate-1 composites and promotes their practical applications in environmental applications.

Acknowledgements The authors grateful acknowledge financial supported by the Scientific Technological Innovation Platform of Fujian Province (2006L2003).

References

1. P. Cosoli, M. Ferrone, S. Pricl, M. Fermeglia, Chem. Eng. J. **145**, 86–92 (2008)
2. M.E. Davis, Nature **417**, 813–821 (2002)
3. V.V. Panic, S.J. Velickovic, Sep. Purif. Technol. **122**, 384–394 (2014)
4. G. Wu, Y. Gao, F.W. Ma, H. Zheng, L.G. Liu, H.Y. Sun, W. Wu, Chem. Eng. J. **271**, 14–22 (2015)
5. C. Zhao, Y. Zhou, D. Ridder, J. Zhai, Y.M. Wei, H.P. Deng, Chem. Eng. J. **248**, 280–289 (2014)
6. J.G. Martínez, M. Johnson, J. Valla, K. Li, J.Y. Ying, Catal. Sci. Technol. **2**, 987–994 (2012)
7. A. Ghorbanpour, J.D. Rimer, L.C. Grabow, ACS Catal. **6**, 2287–2298 (2016)
8. P. Sánchez, F. Dorado, A. Fúnez, V. Jiménez, M.J. Ramos, J.L. Valverde, J. Mol. Catal. A: Chem. **273**, 109–113 (2007)
9. K. Shams, S.J. Mirmohammadi, Microporous Mesoporous Mater. **106**, 268–277 (2007)
10. G. Chandrasekar, M. Hartmann, V. Murugesan, J. Porous Mat. **16**, 175–183 (2009)
11. P. Topka, J. Karban, K. Soukup, K. Jirátová, O. Šolcová, Chem. Eng. J. **168**, 433–440 (2011)
12. L. Itani, V. Valtchev, J. Patarin, S. Rigolet, F. Gao, G. Baudin, Microporous Mesoporous Mater. **138**, 157–166 (2011)
13. P. Vasiliev, F. Akhtar, J. Grins, J. Mouzon, C. Andersson, J. Hedlund, L. Bergsröm, Appl. Mater. Interfaces **2**, 732–737 (2010)
14. F. Akhtar, A. Ojuva, S.K. Wirawan, J. Hedlund, L. Bergström, J. Mater. Chem. **21**, 8822–8828 (2011)
15. F. Akhtar, Q.L. Liu, N. Hedin, L. Bergström, Energ. Environ Sci. **5**, 7664–7767 (2012)
16. F. Akhtar, L. Bergström, J. Am. Ceram. Soc. **94**, 92–98 (2011)
17. A. Nakahira, S. Takezoe, Y. Yamasaki, Y. Sasaki, Y. Ikuhara, J. Am. Ceram. Soc. **90**, 2322–2326 (2007)
18. F. Akhtar, Q.L. Liu, N. Hedin, L. Bergström, Energ. Environ. Sci. **5**, 7664–7673 (2012)
19. B. Singh, A.K. Sinha, J. Mater. Chem. A **2**, 1930–1939 (2014)
20. C.Y. Dai, A.F. Zhang, J.J. Li, K.K. Hou, M. Liu, C.S. Song, X.W. Guo, Chem. Commun. **50**, 4846–4848 (2014)
21. B.S. Li, J.Q. Xu, X. Li, J.J. Liu, S.L. Zuo, Z.Y. Pan, Z.Y. Wu, Mater. Res. Bull. **47**, 1142–1148 (2012)
22. C.A. Morris, M.L. Anderson, R.M. Stroud, C.I. Merzbacher, D.R. Rolison, Science **284**, 622–624 (1999)
23. R. Mechiakh, N.B. Sedrine, R. Chtourou, R. Bensaha, Appl. Surf. Sci. **257**, 670–676 (2010)
24. Q. Zhao, P. Li, D.Q. Li, X.G. Zhou, W.K. Yuan, X.J. Hu, Microporous Mesoporous Mater. **108**, 311–317 (2008)
25. B. Singh, A.K. Sinha, J. Mater. Chem. A. **2**, 1930–1939 (2014)
26. C.S. Chou, F.C. Chou, J.Y. Kang, Powder Technol. **215–216**, 38–45 (2012)
27. M.M. Rashad, A.E. Shalan, M.L. Cantú, M.S.A. Abdel-Mottaleb, Appl. Nanosci. **3**, 167–174 (2013)
28. W.G. Su, J. Zhang, Z.C. Feng, T. Chen, P.L. Ying, C. Li, J. Phys. Chem. C **112**, 7710–7716 (2008)
29. Y.Q. Jing, Y.C. Wang, Y.Z. Gao, H.Q. Li, Y.Y. Cheng, P. Lu, Y.H. Zhang, C. Ma, RSC Adv. **6**, 42495–42510 (2016)